Choroidal hyperpermeability patterns correlate with disease severity in central serous chorioretinopathy: CERTAIN study report 2

Pauleikhoff, L.J.B.; Diederen, R.M.H.; Chang-Wolf, J.M.; Moll, A.C.; Schlingemann, R.O.; Dijk, E.H.C. van; Boon, C.J.F.

Received: 28 November 2023 | Accepted: 13 March 2024

DOI: 10.1111/aos.16679

Acta Ophthalmologica

ORIGINAL ARTICLE

Choroidal hyperpermeability patterns correlate with disease severity in central serous chorioretinopathy: CERTAIN study report 2

Laurenz J. B. Pauleikhoff[1,2] | **Roselie M. H. Diederen**[1] | **Jennifer M. Chang-Wolf**[1,3] | **Annette C. Moll**[1] | **Reinier O. Schlingemann**[1,4,5] | **Elon H. C. van Dijk**[3] | **Camiel J. F. Boon**[1,3]

[1]Department of Ophthalmology, Amsterdam University Medical Centers, Amsterdam, The Netherlands

[2]Department of Ophthalmology, University Medical Center Hamburg-Eppendorf, Hamburg, Germany

[3]Department of Ophthalmology, Leiden University Medical Center, Leiden, The Netherlands

[4]Ocular Angiogenesis Group, Amsterdam University Medical Centers, Amsterdam, The Netherlands

[5]Department of Ophthalmology, University of Lausanne, Jules-Gonin Eye Hospital, Fondation Asile des Aveugles, Lausanne, Switzerland

Correspondence
Camiel J. F. Boon, Department of Ophthalmology, Amsterdam University Medical Centers, PO Box 22660, 1100 DD Amsterdam, The Netherlands.
Email: camiel.boon@amsterdamumc.nl

Funding information
Deutsche Forschungsgemeinschaft, Grant/Award Number: PA 4282/1-1

Abstract

Purpose: Choroidal vascular hyperpermeability (CVH) on indocyanine green angiography (ICGA) is a hallmark feature of central serous chorioretinopathy (CSC). We identified three distinct CVH phenotypes in CSC: uni-focal indistinct signs of choroidal hyperpermeability (uni-FISH) with one focal area of CVH, multiple areas of focal CVH (multi-FISH), and diffuse hyperpermeability covering most of the posterior pole (DISH). This report investigates the distribution of these phenotypes and their association with signs of disease chronicity.

Methods: The CERTAIN study is a monocentric, retrospective study on consecutive CSC patients referred to a large tertiary referral centre that underwent ultra-widefield (UWF) and 55° ICGA. Two independent graders assessed CVH patterns based on mid- to late-phase UWF and 55° ICGA with a third grader acting as referee.

Results: Of the 167 eyes of 91 patients included in this study, 43 (26%) showed uni-FISH, 87 (52%) multi-FISH, and 34 (20%) showed DISH based on UWF ICGA. Median age (40 vs. 45 vs. 57; $p<0.001$) and logMAR visual acuity (0 vs. 0 vs. 0.1, $p<0.001$) differed significantly in-between groups, as did the occurrence of cystoid retinal degeneration (PCRD; 0% vs. 1% vs. 18%, $p<0.001$) or diffuse atrophic RPE alterations (DARA; 0% vs. 17% vs. 29%, $p<0.001$). The same was true when grading was based on 55° ICGA.

Conclusions: The CVH patterns of uni-FISH, multi-FISH, and DISH are typical of CSC. These patterns correlate with established signs of CSC chronicity. Their predictive role in treatment response and prognosis remains to be evaluated.

KEYWORDS
central serous chorioretinopathy, choroidal vascular hyperpermeability, indocyanine green angiography, ultra-widefield ICGA

1 | INTRODUCTION

Central serous chorioretinopathy (CSC) is a common chorioretinopathy that mainly affects men between the ages of 20 and 60 (Pauleikhoff et al., 2021). Its pathognomonic feature is an accumulation of subretinal fluid (SRF) in or around the macula, which can lead to central vision loss, reduced vision-related quality of life, and even legal blindness in long-standing severe cases (Breukink et al., 2017; Mohabati, van Dijk, et al., 2018; Mohabati, van Rijssen, et al., 2018; Mrejen et al., 2019). While the exact cause of CSC is not fully understood, key clinical characteristics involve abnormalities of the choroidal circulation and retinal pigment epithelium (RPE) (van Rijssen, van Dijk, Scholz, Breukink, Blanco-Garavito, Souied, Keunen, et al., 2019; van Rijssen, van Dijk, Scholz, Breukink, Blanco-Garavito, Souied, MacLaren, et al., 2019; van Rijssen, van Dijk, Yzer, et al., 2019).

Choroidal vascular hyperpermeability (CVH), as observed on mid- to late-phase indocyanine green

angiography (ICGA), can be considered a hallmark feature of CSC (Guyer et al., 1994; Prünte & Flammer, 1996). Based on ultra-widefield (UWF) ICGA images of the CERTAIN (Central sErous choRioreTinopAthy wIde-field aNgiography) study, CVH is present in all affected eyes of CSC patients as well as in most unaffected fellow eyes (Pauleikhoff, Diederen, Chang-Wolf, et al., 2023; Pauleikhoff, Diederen, Feenstra, et al., 2023). While CSC patients are classically divided into 2 groups based on fundus fluorescein angiography (FFA) characteristics (focal leakage from a small 'hot-spot' lesion versus more extensive, widespread, and diffuse hyperflorescence and leakage covering larger parts of the retina) (van Rijssen, van Dijk, Scholz, Breukink, Blanco-Garavito, Souied, Keunen, et al., 2019; van Rijssen, van Dijk, Scholz, Breukink, Blanco-Garavito, Souied, MacLaren, et al., 2019; van Rijssen, van Dijk, Yzer, et al., 2019), no such clear-cut definitions yet exist for CVH patterns that can be observed on ICGA.

This report aims to describe distinct CVH patterns that can be observed in CSC and to analyse their correlation with clinical characteristics and signs of disease chronicity.

2 | METHODS

2.1 | Patients

The CERTAIN study is a retrospective study on consecutive CSC patients referred to the Amsterdam University Medical Centers (AUMC) between 01 September 2021 and 30 November 2022, in whom ICGA imaging of sufficient quality was available. Patients underwent a standardized imaging protocol including UWF and 55° ICGA, UWF and 55° fluorescein angiography (FFA), UWF fundus autofluorescence (FAF) as well as enhanced depth optical coherence tomography (EDI-OCT).

We included patients with a clinical diagnosis of CSC based on multimodal imaging criteria described in previous clinical trials performed on this disease (Lotery et al., 2020; Pauleikhoff, Diederen, Chang-Wolf, et al., 2023; Pauleikhoff, Diederen, Feenstra, et al., 2023; van Dijk et al., 2018; van Rijssen et al., 2022). In brief, these criteria include current or previous SRF visible on an EDI-OCT scan and one or more regions of active focal leakage combined with RPE window defects visible on FFA. On 'standard', 55 degree ICGA, hyperfluorescent changes with an indistinct border – characteristic of diseases that are part of the pachychoroid disease spectrum – had to be present (Pang & Freund, 2015; Warrow et al., 2013). The main exclusion criteria included concomitant ophthalmic diseases that did not allow for adequate UWF ICGA imaging (e.g. severe cataract) or other (chorio-)retinal diseases that would impact grading (e.g. proliferative diabetic retinopathy). Eyes with evidence of macular neovascularisation (MNV) on EDI-OCT, optical coherence tomography angiography (OCTA), FFA, and/or ICGA were excluded from the analysis. The study was approved by the local Ethics Committee (LUMC ethics committee vote P14.297) and adhered to the tenets of the Declaration of Helsinki. The full imaging protocol and baseline characteristics of the CERTAIN cohort were published previously (Pauleikhoff, Diederen, Chang-Wolf, et al., 2023; Pauleikhoff, Diederen, Feenstra, et al., 2023).

2.2 | Clinical data acquisition

Clinical characteristics include age, sex, duration of symptoms previous to presentation, and logarithm of the Minimum Angle of Resolution best-corrected visual acuity (logMAR BCVA). A single grader (LJBP) also assessed the presence of posterior cystoid retinal degeneration (PCRD), which was defined as intraretinal spaces without evidence of other causes such as MNV (Mohabati et al., 2020), and the presence of diffuse retinal pigment epithelial atrophy (DARA), defined as a window defect on FFA of at least one disc diameter (Mohabati, van Dijk, et al., 2018; Mohabati, van Rijssen, et al., 2018). Moreover, the FFA leakage pattern was graded as focal leakage from one or multiple distinguishable hotspots or diffuse leakage without clearly distinguishable hotspots (van Rijssen, van Dijk, Scholz, Breukink, Blanco-Garavito, Souied, Keunen, et al., 2019; van Rijssen, van Dijk, Scholz, Breukink, Blanco-Garavito, Souied, MacLaren, et al., 2019; van Rijssen, van Dijk, Yzer, et al., 2019), and subfoveal choroidal thickness was assessed on EDI-OCT. The presence of various signs of venous overload choroidopathy, such as choroidal pachyvessels, intervortex venous anastomoses crossing the watershed zones, and asymmetric venous drainage, were graded by two independent graders (LJBP and JCW) and a third grader in case of disagreement (RMHD). Full results and details on this grading were published previously (Pauleikhoff, Diederen, Chang-Wolf, et al., 2023; Pauleikhoff, Diederen, Feenstra, et al., 2023).

MNV was excluded based on the clinical judgement of the respective experienced retinal specialist (RMHD, ROS, or CJFB) using 55° FFA and ICGA imaging (both Heidelberg Spectralis HRA2, Heidelberg Engineering, Heidelberg, Germany), EDI-OCT (Heidelberg Spectralis OCT, Heidelberg Engineering) as well as 6 × 6 mm swept-source OCTA (ZEISS PLEX Elite 9000, Carl Zeiss Meditec Inc, Jena, Germany).

2.3 | Indocyanine green angiography protocol

All patients underwent simultaneous UWF (Optos California, Optos plc., Dunfermline, United Kingdom) and 55° (Heidelberg Spectralis HRA2, Heidelberg Engineering, Heidelberg, Germany) ICGA as well as FFA within the same session. After immediately subsequent injection of both dyes, multiple UWF images were acquired within the first 4 min. At 3–5 min post-injection, patients were moved to the HRA2 camera, and 55° images were acquired. About 10, 15, and 25 min after indocyanine green injection, additional images were acquired on both devices.

2.4 | Definition of choroidal hyperpermeability patterns

Since CVH originates from the choroidal vasculature, it cannot be linked to a localized leakage point caused by an RPE defect, as is usually the case with FFA leakage. CVH patterns are therefore less clearly demarcated, which is why we refer to them as 'indistinct'. Based on our experience, they can occur in various patterns. These include a relatively small and focal area of CVH or a large, diffuse hyperpermeability covering the majority of the posterior pole. These different phenotypes were termed 'focal indistinct signs of choroidal hyperpermeability' (FISH) or 'diffuse indistinct signs of choroidal hyperpermeability' (DISH), respectively. Since FISH can either be present in a single area of CVH or extend to multiple areas of focal CVH originating from different areas, the terms 'uni-FISH' for a single area of focal CVH and 'multi-FISH' for multiple areas of focal CVH were introduced. DISH, by contrast, was characterized by extensive CVH covering most of the posterior pole, becoming largely confluent in late-phase ICGA. The presence of DISH, however, did not preclude the presence of individual, additional areas of focal CVH in cases of DISH (additional 'satellite lesions'). Imaging examples of uni-FISH, multi-FISH, and DISH are shown in Figures 1–3, respectively.

2.5 | Choroidal hyperpermeability pattern grading

All eyes of patients from the CERTAIN study that showed CVH were included in this study. Based on separate UWF and 55° ICGA images, each eye was graded as showing either uni-FISH, multi-FISH, DISH or no clear CVH detectable. Grading was performed by two independent graders (LJBP, JCW). In case of disagreement, a third grader (CJFB) acted as a referee. Graders were masked for baseline characteristics of the patients such as age, sex, or baseline BCVA. CVH pattern assessments were based on mid- (8–15 min after dye injection) and late-phase (>15 min after dye injection) ICGA images.

2.6 | Potential confounders

To assess the effect of other possible confounders that have been associated with CSC disease severity on CVH patterns, refractive state, autofluorescence pattern, and sensory retinal thickness were also assessed. Since myopia has been associated with some different CSC characteristics compared to emmetropic eyes (Ravenstijn et al., 2021), mean refractive error and lens state (phakia/pseudophakia) was gathered for all patients. Moreover, the presence of hypoautofluorescence on FAF, which has been described as hyper/hypoautofluorescence or descending tracts and was shown to correspond with worse BCVA, was graded by one grader (LJBP) (Han et al., 2020). Since thinner sensory retinal thickness has also been associated with poor BCVA, retinal thickness on EDI-OCT was collected when scans without any sub-/intraretinal fluid were available that allowed for reliable automated thickness measurements (Funatsu et al., 2023; van Rijssen et al., 2018). These factors, as well as the baseline demographic and clinical data collected above, were then integrated into a multinomial regression model with CVH pattern as the dependent, categorical variable. *p*-Values were calculated using the Wald test as described previously, and correcting for multiple testing was applied (UCLA: Statistical Consulting Group., 2021).

2.7 | Statistical analysis

Statistical analysis was performed using R software (Version 4.2.3) ('R: The R Project for Statistical Computing', 2024). Since all continuous variables showed a non-normal distribution, *p*-values were calculated using Kruskal-Wallis tests. To assess which patterns differed significantly, the Mann–Whitney-U test was performed and *p*-values were corrected for multiple testing. Categorical variables were compared using Chi-square statistics, unless zero counts were observed on a variable, in which case Fisher's exact test was performed. Cohen's κ values were calculated to assess inter-grader reliability using the 'irr' package in R. A $p<0.05$ was considered statistically significant. In case multiple tests were performed, Bonferroni correction was applied.

3 | RESULTS

3.1 | Frequency of various hyperpermeability patterns

Based on previous grading, 169 eyes of 91 CSC patients were graded as showing CVH, including 116 symptomatic eyes with current or previous SRF and 53 unaffected fellow eyes. The remaining 9 unaffected fellow eyes showed no CVH. Four eyes were excluded due to a suspected MNV (Pauleikhoff, Diederen, Chang-Wolf, et al., 2023; Pauleikhoff, Diederen, Feenstra, et al., 2023). Upon further investigation for this report, two more eyes were suspected to show secondary MNV, leaving 167 eyes to be analysed in this study.

Based on UWF ICGA, 43/167 eyes (26%) showed a uni-FISH pattern of CVH (Figure 1), 87/167 eyes (52%) showed multi-FISH (Figure 2), and 34/167 eyes (20%) showed DISH (Figure 3), with the remaining 3/167 (2%) patients only showing CVH on 55° ICGA (Table 1). Inter-grader agreement between the grading of these groups was best for uni-FISH (40/43, 93%), 72/87 (83%) for multi-FISH, and 20/34 (59%) for DISH ($p<0.001$). Cohen's κ for inter-grader agreement based on UWF imaging was 0.69, indicating substantial agreement (Landis & Koch, 1977).

3.2 | Differences in baseline characteristics

The median age (inter-quartile range (IQR)) was 40 years (IQR, 35–49) for patients showing uni-FISH, 45 years (IQR, 38–56) for those with multi-FISH, and 57 years

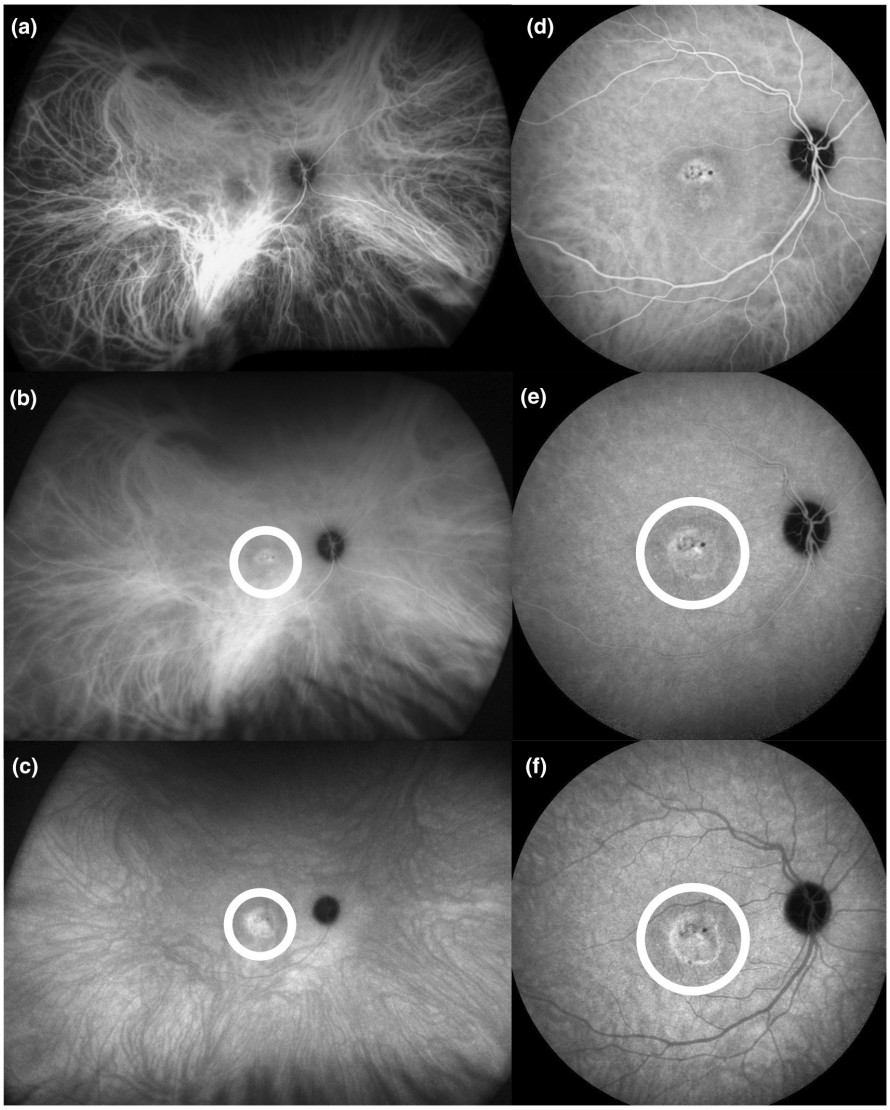

FIGURE 1 Unifocal signs of indistinct choroidal hyperpermeability (uni-FISH). Ultra-widefield (a–c) and 55° (d–f) indocyanine green angiography (ICGA) images of the right eye of a 41-year-old male patient with central serous chorioretinopathy show a single, central area of choroidal vascular hyperpermeability (white circle). Images were acquired consecutively on 55° and ultra-widefield devices within a single imaging session. Images show early-phase ICGA (a), mid-phase ICGA (b, d, e), and late-phase ICGA (c, f).

(IQR, 49−68) for patients with DISH, respectively ($p<0.001$, Figure 4a). The number of female patients per group and the duration of symptoms previous to the date of imaging did not differ significantly between groups (all $p>0.05$). LogMAR BCVA was similar for uni-FISH (0, −0.09 to 0.05) and multi-FISH (0, −0.10 to 0.10) groups, but was significantly worse for DISH (0.1, 0–0.28, $p<0.001$, Figure 4b).

To assess the difference between these groups with regard to disease severity, the presence of signs of CSC chronicity such as PCRD and DARA were also compared (Mohabati et al., 2020; Mohabati, van Dijk, et al., 2018; Mohabati, van Rijssen, et al., 2018). Analysis revealed that PCRD was present in 0/43 (0%) of eyes with uni-FISH, 1/87 eyes (1%) with multi-FISH, and 6/34 (18%) of eyes with DISH ($p<0.001$, Figure 4c). DARA was also not present in eyes showing uni-FISH (0/43, 0%), but was present in 15/87 (17%) of eyes showing multi-FISH, and 10/34 (29%) of eyes showing DISH ($p<0.001$, Figure 4d).

FFA leakage patterns also differed significantly between groups, and focal leakage was more frequently seen in the uni-FISH group (31/43, 72%) compared to multi-FISH (54/87, 62%) and DISH (18/34, 53%). In contrast, diffuse leakage was observed more often in DISH (7/34, 21%) than in multi-FISH (9/87, 10%) and uni-FISH (0/43, 0%), which was, however, not statistically significant after Bonferroni correction ($p=0.03$ across all comparisons). Sensory retinal thickness did also not differ significantly in-between groups (see Table 1).

Multinomial regression analysis, assessing the impact of potential confounders onCVH patterns, found only DARA to be independently associated with the respective pattern, while age, duration of symptoms, logMAR BCVA, presence of PCRD, a hypoautofluorescent FAF pattern, sensory retinal thickness, and subfoveal choroidal thickness were not (see Table S1).

3.3 | Correlation to signs of pachychoroid disease and venous overload

All eyes included in the CERTAIN study had been graded for signs of venous overload choroidopathy

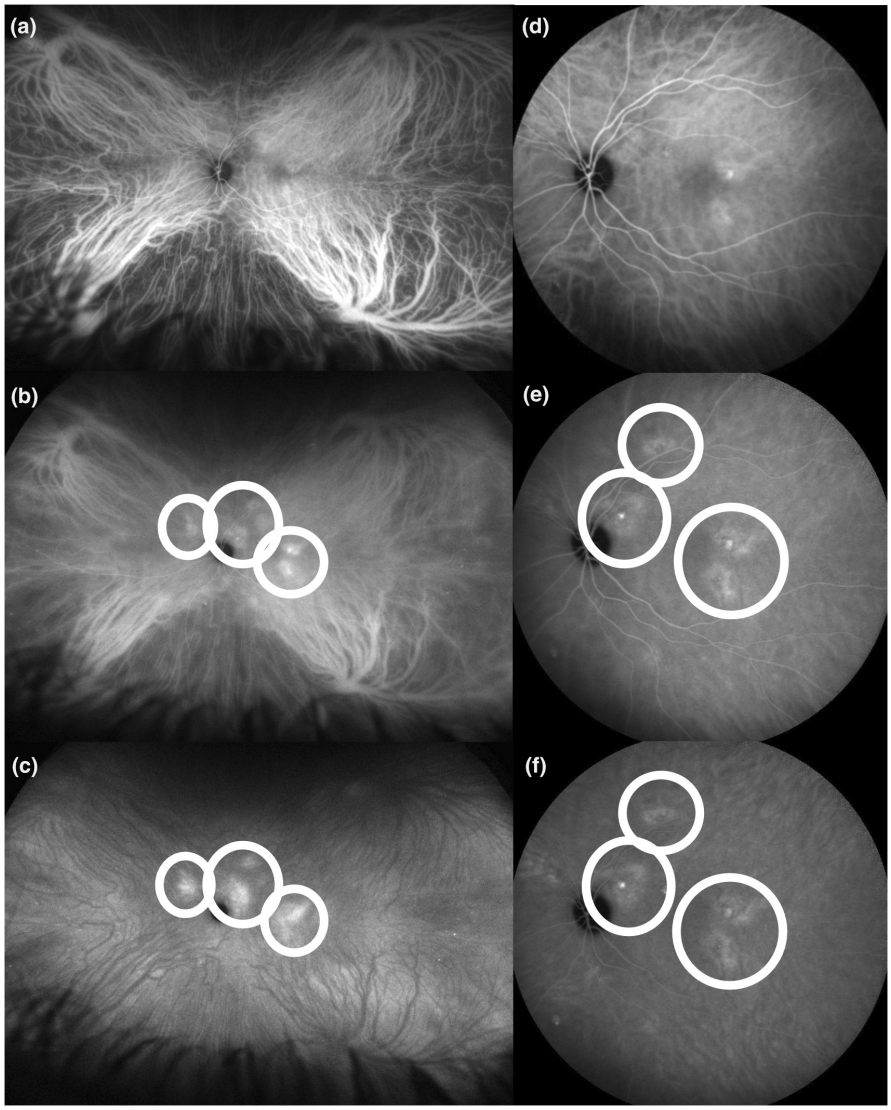

FIGURE 2 Multifocal signs of indistinct choroidal hyperpermeability (multi-FISH). Ultra-widefield (a–c) and 55° (d–f) indocyanine green angiography (ICGA) images of the left eye of a 41-year-old male patient with central serous chorioretinopathy, with multiple areas of choroidal vascular hyperpermeability that expand over time (white circles). Note that these areas do not coalesce and do not cover most of the posterior pole, which contrasts with diffuse indistinct signs of choroidal hyperpermeability (DISH). Images were acquired consecutively on 55° and ultra-widefield devices within a single imaging session. Images show early-phase ICGA (a), mid-phase ICGA (b, d, e), and late-phase ICGA (c, f).

such as presence of pachyvessels, intervortex venous anastomoses, asymmetric venous drainage, and choroidal thickness when possible based on UWF ICGA/OCT imaging. There was no significant difference across the three subgroups with regard to subfoveal choroidal thickness or presence of pachyvessels (Table 1). Intervortex venous anastomoses tended to be present slightly more frequent in uni-FISH (41/43, 95%) and slightly less frequent in DISH (30/34, 88%). At the same time, asymmetric venous drainage was slightly more common in DISH (26/34, 79%) than in uni-FISH (27/43, 68%). However, none of these signs were statistically significantly different between the three groups (all $p > 0.05$).

3.4 | Comparison to 55° ICGA

To assess how readily these CVH patterns can be distinguished based on 55° ICGA, a separate grading was performed based on 55° images only. Based on these images, slightly more patients were graded as showing uni-FISH (38% vs. 26%) while fewer patients were graded as multi-FISH (42% vs. 53%) and a similar proportion was graded as DISH (16% vs. 20%, p between the two gradings = 0.045). A slightly higher proportion of patients did not show CVH on 55° ICGA compared to UWF ICGA (4% vs. 2%, respectively). Grading agreement between UWF and 55° ICGA images was high for uni-FISH (39/43, 91%), and lower for multi-FISH (65/87, 75%) and DISH (26/34, 76%). Cohen's κ, measuring inter-grader agreement, was 0.70 and thus similar to UWF gradings.

Grading based on 55° ICGA images showed the same associations as the grading based on UWF ICGA to baseline characteristics such as patient age, logMAR BCVA, and eyes showing PCRD or DARA (all $p < 0.001$, Table S2). As was true for UWF ICGA, CVH phenotypes on 55° ICGA images did not correlate with either signs of venous overload or choroidal thickness (all $p > 0.05$).

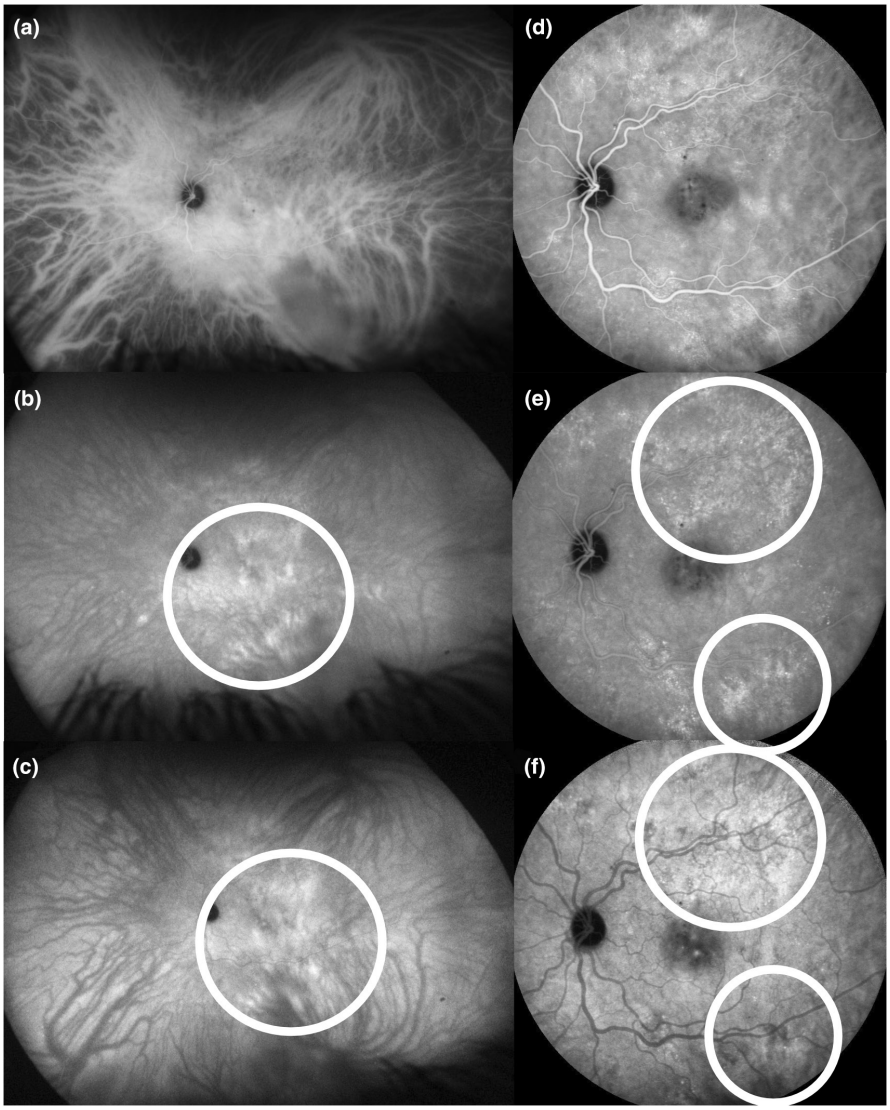

FIGURE 3 Diffuse signs of indistinct choroidal hyperpermeability (DISH). Ultra-widefield (a–c) and 55° (d–f) indocyanine green angiography (ICGA) images of the left eye of a 56-year-old male patient with central serous chorioretinopathy showing diffuse choroidal vascular hyperpermeability coalescing on mid- to late-phase images, covering most of the posterior pole (white circles). Images were acquired consecutively on 55° and ultra-widefield devices within a single imaging session. Images show early-phase ICGA (a), mid-phase ICGA (b, d, e), and late-phase ICGA (c, f).

4 | DISCUSSION

This study proposes a new approach to assess CVH in CSC. Based on both 55° and UWF ICGA, three patterns showing either a single area of focal CVH (uni-FISH), multiple areas of focal CVH (multi-FISH) or diffuse CVH covering most of the posterior pole (DISH) were identified. Moreover, the phenotypes showed a highly differential correlation with previously reported signs of CSC chronicity such as patient age, BCVA, and presence of PCRD or DARA. Based on our results, distinguishing these CVH patterns may aid in a more specific diagnosis and clinical management of CSC patients.

When comparing these different CVH patterns, the extent of CVH increases from uni-FISH (Figure 1) to multi-FISH (Figure 2), and DISH (Figure 3). Similarly, the presence of previously reported signs of disease chronicity also increases in the same order. As reported by Spaide et al. (1996), older patients tend to show more extensive RPE atrophy, and more frequent bilateral involvement and secondary MNV than younger CSC patients. Mohabati, van Dijk, et al. (2018) and Mohabati, van Rijssen, et al. (2018) described a spectrum of severe CSC phenotypes, which encompasses presence of PCRD and widespread DARA, and which shows poorer BCVA outcomes after photodynamic therapy compared to non-severe phenotypes. Single-session photodynamic therapy on eyes with bilateral CSC also showed poorer treatment response than unilateral CSC cases from the PLACE and SPECTRA trials, which may also be attributed to a higher prevalence of DARA and PCRD in this cohort. Moreover, active bilateral CSC may be indicative of a more severe disease (Pauleikhoff, Diederen, Chang-Wolf, et al., 2023; Pauleikhoff, Diederen, Feenstra, et al., 2023). Finally, poorer initial BCVA was associated with a further deterioration in visual acuity during follow-up in CSC patients (Loo et al., 2002). The fact that all these prognostic characteristics differed significantly between the three groups of CVH patterns described here may indicate that the extent of CVH on ICGA correlates with disease severity. Based on the increased presence of

TABLE 1 Clinical characteristics in different choroidal hyperpermeability patterns observed on ultra-widefield indocyanine green angiography.

	Choroidal hyperpermeability pattern based on ultra-widefield ICGA			
	Uni-FISH	**Multi-FISH**	**DISH**	***p***
Patients per group (*n*, %)	43 (26%)	87 (53%)	34 (21%)	
Age (years, median, IQR)	40 (35–49)	45 (38–56)	57 (49–68)	**<0.001**
Female (*n*, %)	9 (21%)	13 (15%)	7 (21%)	0.62
Duration of symptoms (months, median, IQR)	7 (4–12)	7 (4–12)	6 (3–24)	0.82
LogMAR BCVA (median, IQR)	0 (−0.09–0.05)	0 (−0.10–0.10)	0.1 (0–0.28)	**<0.001**
Refractive error (spherical equivalent, median, IQR)	0 (−0.5 to +1.0)	0.1 (−0.4 to +1.1)	0.3 (0 to +1.3)	0.69
Pseudophakic eyes (*n*, %)	3 (7%)	2 (2%)	5 (15%)	0.04
Choroidal thickness (μm, Median, IQR)	365 (309–444)	323 (293–390)	358 (299–437)	0.27
Posterior cystoid retinal degeneration (*n*, %)	0 (0%)	1 (1%)	6 (18%)	**<0.001**
Diffuse RPE atrophy (*n*, %)	0 (0%)	15 (17%)	10 (29%)	**<0.001**
Sensory retinal thickness (μm)	282 (250–298)	268 (237–292)	276 (261–294)	0.55
Fluorescein angiography leakage pattern (*n*, %)				
Focal	31 (72%)	54 (62%)	18 (53%)	0.03
Diffuse	0 (0%)	9 (10%)	7 (21%)	
No leakage	12 (28%)	24 (28%)	9 (26%)	
Presence of				
Pachyvessels (*n*, %)	39 (91%)	78 (90%)	31 (91%)	0.96
Intervortex venous anastomoses (*n*, %)	41 (95%)	79 (91%)	30 (88%)	0.51
Asymmetric venous drainage (*n*, %)	27 (68%)	60 (74%)	26 (79%)	0.54

Note: *p*-Values were calculated using three-grouped Kruskal-Wallis test for continuous and Chi-square test for categorical variables. In case of 0 observations in one group, Fisher's exact test was performed instead. Significant associations ($p<0.005$ after Bonferroni correction) are highlighted in bold.

Abbreviations: DISH, diffuse indistinct signs of choroidal hyperpermeability; FISH, focal indistinct signs of choroidal hyperpermeability; ICGA, indocyanine green angiography; IQR, inter-quartile range; logMAR BCVA, logarithm of the Minimum Angle of Resolution best-corrected visual acuity; RPE, retinal pigment epithelium.

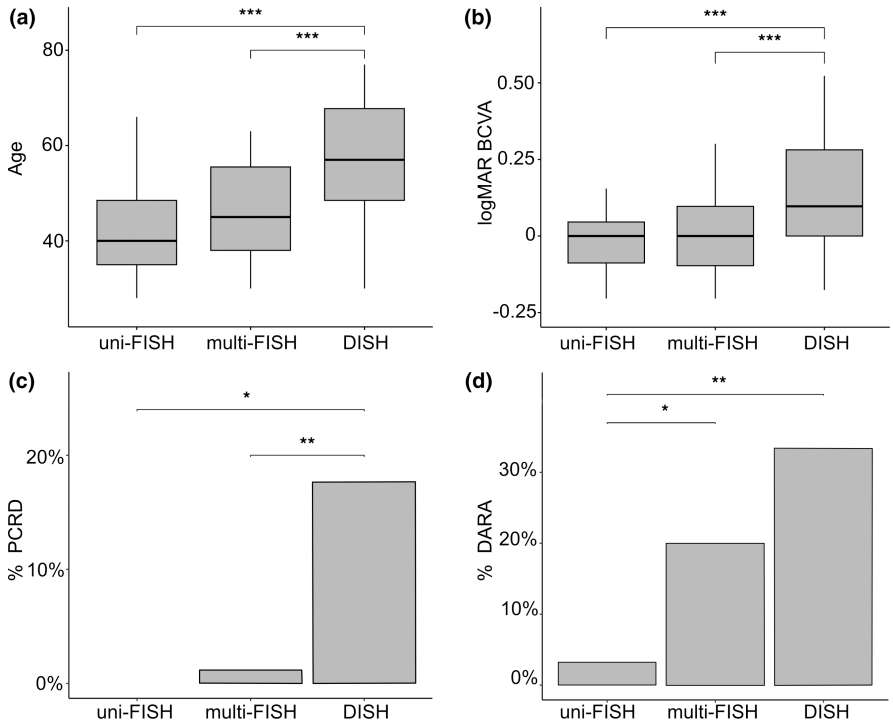

FIGURE 4 Baseline characteristics significantly associated with choroidal hyperpermeability pattern. Age in years (a), logarithm of the Minimum Angle of Resolution best-corrected visual acuity (logMAR BCVA, b), proportion of eyes showing posterior cystoid retinal degeneration (PCRD, c), and proportion of eyes showing diffuse atrophy of the retinal pigment epithelium (DARA, d) for uni-FISH, multi-FISH, and DISH groups, respectively. Subgroups were compared using the Mann–Whitney-U test. *$p<0.02$, **$p<0.003$, ***$p<0.0003$ (after applying Bonferroni correction).

DARA and given the fact that this was the only factor independently associated with CVH patterns, it could also be hypothesized that extensive CVH has a deleterious effect on RPE health. Whether CVH patterns correlate with clinical (treatment) outcomes remains to be established in future studies.

The results of this report also reiterate our previous finding that one or more areas of indistinct CVH on ICGA are a hallmark feature of CSC, being present in all affected eyes and even in 85% of previously unaffected fellow eyes of CSC patients (Pauleikhoff, Diederen, Chang-Wolf, et al., 2023; Pauleikhoff, Diederen, Feenstra, et al., 2023). This high sensitivity may aid the often challenging differential diagnosis of CSC, including a broad spectrum of diseases (van Dijk & Boon, 2021). Since CSC is often considered part of the pachychoroid disease spectrum, which describes a range of diseases associated with an abnormal, thickened choroid (Cheung et al., 2019), some reports suggested that a thickened subfoveal choroid ('pachychoroid') of more than 300 μm or 350 μm thickness could hint at a diagnosis of CSC (Spaide, 2021). In our previous CERTAIN report, we already noted that 26% of CSC eyes did not show a subfoveal choroidal thickness of >300 μm, which make this criterion far less specific than presence of CVH (Pauleikhoff, Diederen, Chang-Wolf, et al., 2023; Pauleikhoff, Diederen, Feenstra, et al., 2023). In the current study, we also did not see any difference in choroidal thickness between the three CVH patterns. Moreover, healthy patients can often show a relatively thick choroid without any pathological changes (Ikuno et al., 2010), while CVH is rarely found in healthy controls, thus making it a more specific sign of the disease (Bacci et al., 2022). The same holds true for other signs of venous overload such as intervortex venous anastomoses, which were observed in between 35% (Bacci et al., 2022) and 58% (Fernández-Vigo et al., 2023) of healthy controls and can thus not be regarded a pathologic sign only observed in diseases that are part of the pachychoroid spectrum (Funatsu et al., 2022; Sonoda et al., 2021). Based on these results, CVH appears to be a more meaningful diagnostic feature of CSC than either a thickened choroid or signs of venous overload. The three distinct CVH patterns described in this report may even further this advantage, since they were present in 98% of CSC eyes showing CVH. Since CVH was also reported to occur in other pachychoroid diseases (Cheung et al., 2018, 2019; Ersoz et al., 2018), future reports may investigate whether these diseases exhibit similar CVH patterns to the ones described in this report.

The categories we propose in this paper may also aid in the classification of CSC, which is still a contentious topic. Traditionally, CSC is classified as either acute or chronic CSC based on the duration of SRF (Daruich et al., 2015; Pauleikhoff et al., 2021; van Rijssen, van Dijk, Scholz, Breukink, Blanco-Garavito, Souied, Keunen, et al., 2019; van Rijssen, van Dijk, Scholz, Breukink, Blanco-Garavito, Souied, MacLaren, et al., 2019; van Rijssen, van Dijk, Yzer, et al., 2019). A more comprehensive definition is warranted, since the exact disease duration can be difficult to establish and may not correlate with clinical outcomes. Large randomized controlled treatment trials such as PLACE and SPECTRA therefore used a definition of chronic CSC as SRF on OCT, 1 or more regions of active leakage on FFA combined with RPE window defects visible on FFA, hyperfluorescent changes on ICGA as well as SRF/subjective visual symptoms for at least 6 weeks to define eligibility (van Dijk et al., 2018; van Rijssen et al., 2022). Recently, a new classification into simple, complex, and atypical CSC cases has been proposed, focusing more on multimodal imaging findings and less on disease duration (Chhablani et al., 2020). Thus far, however, only a moderate inter-grader agreement was observed when using this classification (Chhablani et al., 2022). Since the CVH patterns described in this report showed a substantial inter-grader agreement (Cohen's κ 0.69 and 0.70, respectively) and correlate with many signs of disease chronicity, refining current CSC definitions by including ICGA patterns may further improve their reproducibility and clinical validity.

As part of this report, we also investigated how CVH patterns correlate with signs of venous overload choroidopathy (Spaide, Gemmy Cheung, et al., 2021; Spaide, Ledesma-Gil, et al., 2021). This concept proposes that increased choroidal venous pressure leads to enlarged choroidal veins ('pachyvessels', which can also be seen on OCT), asymmetric drainage of choroidal vortex vein quadrants, and consecutive anastomoses between vortex veins (intervortex venous anastomoses) (Bacci et al., 2022; Brinks et al., 2022; Ramtohul et al., 2022; Spaide, Gemmy Cheung, et al., 2021; Spaide, Ledesma-Gil, et al., 2021). Interestingly, while the three CVH patterns described in this report correlated with signs of disease chronicity, such as BCVA and age, they did not differ with regard to signs of venous overload. While the concept of venous overload choroidopathy may reveal important insights into CSC pathogenesis, the current study suggests that CVH patterns may be better suited to assess individual CSC phenotypes than the degree of signs of venous overload and congestion observed on UWF ICGA. Whether the location of areas of CVH correlates with other anatomical changes, such as neurosensory or pigment epithelial detachment, remains to be elucidated.

Our data also show that grading of CVH patterns can be performed based both on UWF and 55° ICGA images. Our grading on 55° imaging showed an excellent agreement with UWF ICGA grading for presence of uni-FISH (91%), and slightly lower agreement for multi-FISH (75%) and DISH (76%). Due to its wide-angle nature, UWF ICGA may reveal additional areas of focal CVH that may be missed on 55° ICGA, leading to more uni-FISH (38% based on 55° vs. 26% based on UWF) and fewer multi-FISH (42% based on 55° vs. 53% based on UWF) cases on 55° imaging. Moreover, no clear CVH was detectable in only 2% of UWF images compared to 4% of 55° images. This discrepancy is most likely also due to peripheral areas of CVH not covered by 55° ICGA, while, on the other hand, small uni-FISH lesions may sometimes be difficult to detect on UWF imaging. Importantly, however, gradings on UWF and 55° ICGA still showed the same association with well-established signs of CSC chronicity. From a clinical perspective, we

therefore believe that both imaging modalities can be used reliably to assess CVH patterns.

Limitations of this study include (1) its retrospective design and (2) the grader-dependent assessment of CVH patterns. Especially discerning extensive multi-FISH phenotypes with many focal areas of CVH from a DISH pattern covering most of the posterior pole sometimes proved difficult (also see Figure S1). These shortcomings were addressed by (1) analysing consecutive CSC patients and providing a detailed patient flow of all eligible patients (Pauleikhoff, Diederen, Chang-Wolf, et al., 2023; Pauleikhoff, Diederen, Feenstra, et al., 2023) and (2) the grading being performed by two independent, masked graders and a third grader acting as referee in case of disagreement. Moreover, all graders were provided with written definitions and imaging examples of the three phenotypes to ensure consistent grading.

In conclusion, our report highlights the role of different CVH patterns in diagnosing CSC and assessing its extent and severity. We also show that these patterns can be reliably detected both on UWF and 55° ICGA, which may aid clinical management of CSC patients. Future studies are needed to investigate how these patterns relate to (treatment) outcomes in CSC, and whether CVH patterns can also be found in other diseases that are part of the pachychoroid disease spectrum.

ACKNOWLEDGEMENTS

L. J. B. Pauleikhoff was supported by the Deutsche Forschungsgemeinschaft (DFG; Grant PA 4282/1-1). This funding organisation provided unrestricted grants and had no role in the design or conduct of this research.

ORCID

Laurenz J. B. Pauleikhoff https://orcid.org/0000-0001-7671-8391
Roselie M. H. Diederen https://orcid.org/0000-0001-9708-2898
Annette C. Moll https://orcid.org/0000-0002-9313-8345
Camiel J. F. Boon https://orcid.org/0000-0002-6737-7932

REFERENCES

Bacci, T., Oh, D.J., Singer, M., Sadda, S. & Freund, K.B. (2022) Ultra-widefield indocyanine green angiography reveals patterns of choroidal venous insufficiency influencing pachychoroid disease. *Investigative Ophthalmology & Visual Science*, 63, 17.

Breukink, M.B., Dingemans, A.J., den Hollander, A.I., Keunen, J.E., MacLaren, R., Fauser, S. et al. (2017) Chronic central serous chorioretinopathy: long-term follow-up and vision-related quality of life. *Clinical Ophthalmology*, 11, 39–46.

Brinks, J., van Dijk, E.H.C., Meijer, O.C., Schlingemann, R.O. & Boon, C.J.F. (2022) Choroidal arteriovenous anastomoses: a hypothesis for the pathogenesis of central serous chorioretinopathy and other pachychoroid disease spectrum abnormalities. *Acta Ophthalmologica*, 100, 946–959.

Cheung, C.M.G., Lai, T.Y.Y., Ruamviboonsuk, P., Chen, S.J., Chen, Y., Freund, K.B. et al. (2018) Polypoidal choroidal vasculopathy: definition, pathogenesis, diagnosis, and management. *Ophthalmology*, 125, 708–724.

Cheung, C.M.G., Lee, W.K., Koizumi, H., Dansingani, K., Lai, T.Y.Y. & Freund, K.B. (2019) Pachychoroid disease. *Eye*, 33, 14–33.

Chhablani, J., Behar-Cohen, F. & Central Serous Chorioretinopathy International Group. (2022) Validation of central serous chorioretinopathy multimodal imaging-based classification system. *Graefe's Archive for Clinical and Experimental Ophthalmology*, 260, 1161–1169.

Chhablani, J., Cohen, F.B. & Central Serous Chorioretinopathy International Group. (2020) Multimodal imaging-based central serous chorioretinopathy classification. *Ophthalmology Retina*, 4, 1043–1046.

Daruich, A., Matet, A., Dirani, A., Bousquet, E., Zhao, M., Farman, N. et al. (2015) Central serous chorioretinopathy: recent findings and new physiopathology hypothesis. *Progress in Retinal and Eye Research*, 48, 82–118.

Ersoz, M.G., Arf, S., Hocaoglu, M., Sayman Muslubas, I. & Karacorlu, M. (2018) Indocyanine green angiography of pachychoroid pigment epitheliopathy. *Retina*, 38, 1668–1674.

Fernández-Vigo, J.I., Rego-Lorca, D., Moreno-Morillo, F.J., Burgos-Blasco, B., Valverde-Megías, A., Méndez-Hernández, C. et al. (2023) Intervortex venous anastomosis in the macula in central serous chorioretinopathy imaged by en face optical coherence tomography. *Journal of Clinical Medicine*, 12, 2088.

Funatsu, R., Sonoda, S., Terasaki, H., Shiihara, H., Mihara, N., Horie, J. et al. (2022) Choroidal morphologic features in central serous chorioretinopathy using ultra-widefield optical coherence tomography. *Graefe's Archive for Clinical and Experimental Ophthalmology*, 261, 971–979.

Funatsu, R., Terasaki, H., Sonoda, S., Shiihara, H., Mihara, N. & Sakamoto, T. (2023) A photodynamic therapy index for central serous chorioretinopathy to predict visual prognosis using pretreatment factors. *American Journal of Ophthalmology*, 253, 86–95.

Guyer, D.R., Yannuzzi, L.A., Slakter, J.S., Sorenson, J.A., Ho, A. & Orlock, D. (1994) Digital indocyanine green videoangiography of central serous chorioretinopathy. *Archives of Ophthalmology*, 112, 1057–1062.

Han, J., Cho, N.S., Kim, K., Kim, E.S., Kim, D.G., Kim, J.M. et al. (2020) Fundus autofluorescence patterns in central serous chorioretinopathy. *Retina*, 40, 1387–1394.

Ikuno, Y., Kawaguchi, K., Nouchi, T. & Yasuno, Y. (2010) Choroidal thickness in healthy Japanese subjects. *Investigative Ophthalmology & Visual Science*, 51, 2173–2176.

Landis, J.R. & Koch, G.G. (1977) The measurement of observer agreement for categorical data. *Biometrics*, 33, 159–174.

Loo, R.H., Scott, I.U., Flynn, H.W., Gass, J.D.M., Murray, T.G., Lewis, M.L. et al. (2002) Factors associated with reduced visual acuity during long-term follow-up of patients with idiopathic central serous chorioretinopathy. *Retina*, 22, 19–24.

Lotery, A., Sivaprasad, S., O'Connell, A., Harris, R.A., Culliford, L., Ellis, L. et al. (2020) Eplerenone for chronic central serous chorioretinopathy in patients with active, previously untreated disease for more than 4 months (VICI): a randomised, double-blind, placebo-controlled trial. *The Lancet*, 395, 294–303.

Mohabati, D., Hoyng, C.B., Yzer, S. & Boon, C.J.F. (2020) Clinical characteristics and outcome of posterior cystoid macular degeneration in chronic central serous chorioretinopathy. *Retina*, 40, 1742–1750.

Mohabati, D., van Dijk, E.H., van Rijssen, T.J., de Jong, E.K., Breukink, M.B., Martinez-Ciriano, J.P. et al. (2018) Clinical spectrum of severe chronic central serous chorioretinopathy and outcome of photodynamic therapy. *Clinical Ophthalmology*, 12, 2167–2176.

Mohabati, D., van Rijssen, T.J., van Dijk, E.H., Luyten, G.P., Missotten, T.O., Hoyng, C.B. et al. (2018) Clinical characteristics and long-term visual outcome of severe phenotypes of chronic central serous chorioretinopathy. *Clinical Ophthalmology*, 12, 1061–1070.

Mrejen, S., Balaratnasingam, C., Kaden, T.R., Bottini, A., Dansingani, K., Bhavsar, K.V. et al. (2019) Long-term visual outcomes and causes of vision loss in chronic central serous chorioretinopathy. *Ophthalmology*, 126, 576–588.

Pang, C.E. & Freund, K.B. (2015) Pachychoroid neovasculopathy. *Retina*, 35, 1–9.

Pauleikhoff, L., Agostini, H. & Lange, C. (2021) Central serous chorioretinopathy. *Der Ophthalmologe*, 118, 967–980.

Pauleikhoff, L.J.B., Diederen, R.M.H., Chang-Wolf, J.M., Moll, A.C., Schlingemann, R.O., van Dijk, E.H.C. et al. (2023) Choroidal

vascular changes on ultra-widefield indocyanine green angiography in central serous chorioretinopathy: CERTAIN study report 1. *Ophthalmology Retina*, 8, 254–263.

Pauleikhoff, L.J.B., Diederen, R.M.H., Feenstra, H., Schlingemann, R.O., van Dijk, E.H.C. & Boon, C.J.F. (2023) Single-session bilateral reduced-settings photodynamic therapy for bilateral chronic central serous chorioretinopathy. *Retina*, 43, 1356–1363.

Prünte, C. & Flammer, J. (1996) Choroidal capillary and venous congestion in central serous chorioretinopathy. *American Journal of Ophthalmology*, 121, 26–34.

R: The R Project for Statistical Computing. (2024) https://www.r-project.org/ [Accessed 25th March 2024].

Ramtohul, P., Cabral, D., Oh, D., Galhoz, D. & Freund, K.B. (2022) En face ultrawidefield OCT of the vortex vein system in central serous chorioretinopathy. *Ophthalmology Retina*, 7, 346–353.

Ravenstijn, M., van Dijk, E.H.C., Haarman, A.E.G., Kaden, T.R., Vermeer, K.A., Boon, C.J.F. et al. (2021) Myopic presentation of central serous chorioretinopathy. *Retina*, 41, 2472–2478.

Sonoda, S., Shiihara, H., Terasaki, H., Kakiuchi, N., Funatsu, R., Tomita, M. et al. (2021) Artificial intelligence for classifying uncertain images by humans in determining choroidal vascular running pattern and comparisons with automated classification between artificial intelligence. *PLoS One*, 16, e0251553.

Spaide, R.F. (2021) The ambiguity of pachychoroid. *Retina*, 41, 231–237.

Spaide, R.F., Campeas, L., Haas, A., Yannuzzi, L.A., Fisher, Y.L., Guyer, D.R. et al. (1996) Central serous chorioretinopathy in younger and older adults. *Ophthalmology*, 103, 2070–2079; discussion 2079–2080.

Spaide, R.F., Gemmy Cheung, C.M., Matsumoto, H., Kishi, S., Boon, C.J.F., van Dijk, E.H.C. et al. (2021) Venous overload choroidopathy: a hypothetical framework for central serous chorioretinopathy and allied disorders. *Progress in Retinal and Eye Research*, 86, 100973.

Spaide, R.F., Ledesma-Gil, G. & Gemmy Cheung, C.M. (2021) Intervortex venous anastomosis in pachychoroid-related disorders. *Retina*, 41, 997–1004.

UCLA: Statistical Consulting Group. (2021) *Multinomial logistic regression*.

van Dijk, E.H.C. & Boon, C.J.F. (2021) Serous business: delineating the broad spectrum of diseases with subretinal fluid in the macula. *Progress in Retinal and Eye Research*, 84, 100955.

van Dijk, E.H.C., Fauser, S., Breukink, M.B., Blanco-Garavito, R., Groenewoud, J.M.M., Keunen, J.E.E. et al. (2018) Half-dose photodynamic therapy versus high-density subthreshold micropulse laser treatment in patients with chronic central serous chorioretinopathy: the PLACE trial. *Ophthalmology*, 125, 1547–1555.

van Rijssen, T.J., Mohabati, D., Dijkman, G., Theelen, T., de Jong, E.K., van Dijk, E.H.C. et al. (2018) Correlation between redefined optical coherence tomography parameters and best-corrected visual acuity in non-resolving central serous chorioretinopathy treated with half-dose photodynamic therapy. *PLoS One*, 13, e0202549.

van Rijssen, T.J., van Dijk, E.H.C., Scholz, P., Breukink, M.B., Blanco-Garavito, R., Souied, E.H. et al. (2019) Focal and diffuse chronic central serous chorioretinopathy treated with half-dose photodynamic therapy or subthreshold micropulse laser: PLACE trial report no. 3. *American Journal of Ophthalmology*, 205, 1–10.

van Rijssen, T.J., van Dijk, E.H.C., Scholz, P., Breukink, M.B., Blanco-Garavito, R., Souied, E.H. et al. (2019) Patient characteristics of untreated chronic central serous chorioretinopathy patients with focal versus diffuse leakage. *Graefe's Archive for Clinical and Experimental Ophthalmology*, 257, 1419–1425.

van Rijssen, T.J., van Dijk, E.H.C., Tsonaka, R., Feenstra, H.M.A., Dijkman, G., Peters, P.J.H. et al. (2022) Half-dose photodynamic therapy versus Eplerenone in chronic central serous chorioretinopathy (SPECTRA): a randomized controlled trial. *American Journal of Ophthalmology*, 233, 101–110.

van Rijssen, T.J., van Dijk, E.H.C., Yzer, S., Ohno-Matsui, K., Keunen, J.E.E., Schlingemann, R.O. et al. (2019) Central serous chorioretinopathy: towards an evidence-based treatment guideline. *Progress in Retinal and Eye Research*, 73, 100770.

Warrow, D.J., Hoang, Q.V. & Freund, K.B. (2013) Pachychoroid pigment epitheliopathy. *Retina*, 33, 1659–1672.

SUPPORTING INFORMATION

Additional supporting information can be found online in the Supporting Information section at the end of this article.

How to cite this article: Pauleikhoff, L.J.B., Diederen, R.M.H., Chang-Wolf, J.M., Moll, A.C., Schlingemann, R.O., van Dijk, E.H.C. et al. (2024) Choroidal hyperpermeability patterns correlate with disease severity in central serous chorioretinopathy: CERTAIN study report 2. *Acta Ophthalmologica*, 102, e946–e955. Available from: https://doi.org/10.1111/aos.16679